



On-Demand Sequencing for Your Lab, Your Samples, Your Schedule




Avoid batching samples or depending on sequencing services with the Spectrum Compact CE System, a personal, benchtop instrument for Sanger sequencing and 6-dye fragment analysis featuring an easy-to-use touch screen, remote access software, plug-and-play prefilled consumables and unlimited support.

Discover the possibilities:

promega.com/SpectrumCompactCE



TFIIH stabilization recovers the DNA repair and transcription dysfunctions in thermo-sensitive trichothiodystrophy

Manuela Lanzafame¹ | Tiziana Nardo¹ | Roberta Ricotti¹ | Chiara Pantaleoni² | Stefano D'Arrigo² | Franco Stanzial³ | Francesco Benedicenti³ | Mary A. Thomas⁴ | Miria Stefanini¹ | Donata Orioli¹ | Elena Botta¹ 

¹Istituto di Genetica Molecolare "Luigi Luca Cavalli-Sforza" (IGM) CNR, Pavia, Italy

²Dipartimento Neuroscienze Pediatriche, Fondazione IRCCS Istituto Neurologico Carlo Besta, Milano, Italy

³Genetic Counseling Service, Department of Pediatrics, Regional Hospital of Bolzano, Bolzano, Italy

⁴Department of Medical Genetics, Cumming, School of Medicine, University of Calgary, Calgary, Alberta, Canada

Correspondence

Elena Botta and Donata Orioli, Istituto di Genetica Molecolare "Luigi Luca Cavalli-Sforza" (IGM) CNR, Via Abbiategrosso 207, 27100 Pavia, Italy.
Email: elena.botta@igm.cnr.it and donata.orioli@igm.cnr.it

Funding information

Associazione Italiana per la Ricerca sul Cancro

Abstract

Trichothiodystrophy (TTD) is a rare hereditary disease whose prominent feature is brittle hair. Additional clinical signs are physical and neurodevelopmental abnormalities and in about half of the cases hypersensitivity to UV radiation. The photosensitive form of TTD (PS-TTD) is most commonly caused by mutations in the *ERCC2/XPD* gene encoding a subunit of the transcription/DNA repair complex TFIIH. Here we report novel *ERCC2/XPD* mutations affecting proper protein folding, which generate thermo-labile forms of XPD associated with thermo-sensitive phenotypes characterized by reversible aggravation of TTD clinical signs during episodes of fever. In patient cells, the newly identified XPD variants result in thermo-instability of the whole TFIIH complex and consequent temperature-dependent defects in DNA repair and transcription. Improving the protein folding process by exposing patient cells to low temperature or to the chemical chaperone glycerol allowed rescue of TFIIH thermo-instability and a concomitant recovery of the complex activities. Besides providing a rationale for the peculiar thermo-sensitive clinical features of these new cases, the present findings demonstrate how variations in the cellular concentration of mutated TFIIH impact the cellular functions of the complex and underlie how both quantitative and qualitative TFIIH alterations contribute to TTD clinical features.

KEYWORDS

ERCC2 mutations, TFIIH, thermo-sensitivity, trichothiodystrophy, XPD

1 | INTRODUCTION

Trichothiodystrophy (TTD) is a rare hereditary pathological condition whose diagnostic feature is sulfur-deficient brittle hair characterized by dark and light alternate bands (tiger tail pattern) on polarized microscopy. Hair alterations are associated with a broad spectrum of clinical symptoms of varying severity, including growth and neurodevelopmental issues, short stature, ichthyotic skin, nail dysplasia, decreased fertility, recurrent infections, unusual facial features and signs of premature ageing (Faghri et al., 2008). About half of TTD

cases also exhibit cutaneous sun sensitivity that is associated with cell hypersensitivity to ultraviolet (UV) light. These patients are defined photosensitive TTD (PS-TTD; MIM# 601675, 616390, 616395) and carry bi-allelic mutations in *ERCC2/XPD*, *ERCC3/XPB*, or *GTF2H5/TTDA* genes, encoding distinct subunits of the general transcription factor IIIH (TFIIH). Besides transcription, TFIIH plays a key role in nucleotide excision repair (NER) (Compe & Egly, 2016; Rimel & Taatjes, 2018; Tsutakawa et al., 2020), the only DNA repair pathway that in mammalian cells removes bulky DNA adducts induced by UV light. Alterations in XPD and XPB subunits of TFIIH

have been also linked to the hereditary disorder xeroderma pigmentosum (XP) characterized by a high incidence of cancer formation in the sun-exposed areas of the skin (Ferri et al., 2020). Defects in NER can explain the high skin cancer proneness in XP patients while impaired transcription likely contributes to the multisystem clinical features of PS-TTD. Multiple in vitro and in vivo data support this notion, including impaired basal transcription activity of recombinant TFIIH complexes carrying PS-TTD mutations (Dubaele et al., 2003) as well as the recent finding that mutations in another basal transcription factor, the TFIIIE complex, also lead to TTD clinical features with no NER defects (Kuschal et al., 2016; Theil et al., 2017). Several studies in the mouse model or in patient cells have also demonstrated the relevance for disease pathogenesis of TFIIH in gene expression regulation (Arseni et al., 2015; Compe et al., 2005, 2007; Lombardi et al., 2021; Orioli et al., 2013). In addition, all PS-TTD mutations have been shown to affect the stability of the TFIIH complex, thus resulting in reduced TFIIH cellular amounts (Botta et al., 2002; Vermeulen et al., 2000, 2001) that might be rate limiting for specific genes in certain cells and/or tissues relevant for the disease.

More than 80% of PS-TTD cases are associated with alterations in the XPD helicase subunit of TFIIH. These patients display remarkably wide phenotypic heterogeneity with striking differences in both the progression and severity of the disease (Faghri et al., 2008; Orioli & Stefanini, 2019). Here, we report novel changes in XPD related to thermo-sensitive clinical features that appear to reflect protein folding alterations. Five PS-TTD/XP-D patients (from three unrelated families) who were referred to the laboratory presented medical histories notable for fever-dependent aggravation of typical TTD symptoms. During febrile states, they exhibited sudden loss of brittle hair which regrew after recovery. Transient difficulty with walking and balance and skin peeling were also observed concurrently with body temperature increase. We show that these patients carry still unreported mutations in the *ERCC2/XPD* gene and demonstrate that the new mutations generate thermo-sensitive forms of XPD protein resulting in temperature-dependent instability of the whole TFIIH complex. As a consequence, patient cells show temperature-dependent worsening of NER and transcription dysfunctions. By improving protein folding, thermo-instability of the mutant XPD subunits can be partially rescued with a concomitant recovery of TFIIH cellular amounts and activities. Thus, patient cells with thermo-sensitive mutations offer a unique opportunity to directly evaluate the influence of quantitative variations on TFIIH efficiency.

2 | MATERIALS AND METHODS

2.1 | Patients, cell culture conditions, and complementation analysis

Individuals investigated in this study followed the protocols approved by CNR Ethics and Integrity Committee. The study was performed on

primary skin fibroblasts from the TTD32PV, TTD34PV, TTD35PV, TTD37PV, and TTD38PV patients (Supporting Information: Table S1) and the C3PV healthy donor. Fibroblasts from TTD8PV (XP-D), TTD14PV (TTD-A), TTD20PV (XP-D), TTD22PV (XP-D), and XP5PV (XP-C) were used as reference strains in complementation studies (Botta et al., 1998, 2009; Chavanne et al., 2000; Giglia-Mari et al., 2004). Investigations on the effect of temperature were extended to primary fibroblasts of the TTD8PV, TTD12PV, TTD22PV, and TTD23PV patients (Supporting Information: Table S1).

Fibroblasts were cultured in Dulbecco's modified Eagle's medium (DMEM) medium (DMEM High Glucose with L-glutamine; EuroClone) supplemented with 10% fetal bovine serum (FBS; Lonza) and 1% penicillin-streptomycin (EuroClone) at 37°C and 5% CO₂.

The genetic defect responsible for UV hypersensitivity was defined by complementation assays. Procedures are those routinely used in our laboratory and have been described elsewhere (Stefanini et al., 1992, 1993).

2.2 | Treatments

Temperature shift experiments were carried out on parallel cultures of 5×10^5 fibroblasts in 100 mm Petri dishes. Cells were incubated at 37°C for 48 h and then either maintained at 37°C or moved to 32°C or 41°C for additional 12 h before processing.

For glycerol treatment, 5×10^5 fibroblasts were cultured under standard conditions for 2 days. Medium containing 0.66 M glycerol (BDH Prolabo) was then added to culture dishes and temperature shift experiments were performed.

UV irradiation was performed using a Philips TUV 15 W lamp emitting predominantly 254 nm light (i.e., UVC) and giving a dose rate of 2 J/m²/s. The UV intensity was measured before cell exposure with a calibrated radiometer (WXL Radiometer, Vilber Lourmat).

2.3 | Unscheduled DNA synthesis (UDS) and overall RNA synthesis rate (RS)

UDS and RS were analyzed by autoradiography, as previously described (Stefanini et al., 1986, 1996). Briefly, for UDS analysis, cells were seeded in dishes provided with a coverslip, grown under standard conditions for 2 days, and then exposed to a UV dose of 20 J/m², incubated in a medium containing 10 μCi/ml ³H-thymidine (Perkin Elmer Life Sciences, specific activity 20 Ci/mmol) for 3 h, washed in PBS, and fixed with Bouin's solution. For RS analysis, cells were seeded in dishes provided with a coverslip in medium with low serum (1% FBS), grown for 3 days, and then incubated in medium containing 10 μCi/ml ³H-uridine (NER Radiochemicals, specific activity 26.4 Ci/mmol) for 1 h and processed as described above. Autoradiographic preparations were performed using a photographic emulsion (Ilford K2). After 2–3 days at 4°C, the slides were developed and stained with May-Grunwald (BDH Prolabo) and Giemsa (BDH Prolabo) solutions. UDS and RS were evaluated by counting the

number of autoradiographic grains on at least 25 nuclei of G1/G2 phase cells.

2.4 | Sequencing of ERCC2 gene

The complete coding region of *ERCC2* (GenBank reference mRNA sequence NM_000400.4) was analyzed by sequencing of PCR-amplified cDNA. Identified variants were also investigated in the corresponding genomic DNA regions (GenBank reference genomic sequence NG_007067.2, range 5001–24197).

Total RNA was extracted from patient fibroblasts using the RNeasy Mini kit (Qiagen) according to the manufacturer's instructions. Genomic DNA was prepared from parent blood withdrawals by the salting out method. PCR amplification and sequencing were carried out as previously described (Botta et al., 2009). Primer sequences are given in Supporting Information: Table S2.

2.5 | Quantitative real-time PCR (qRT-PCR)

Total RNA was extracted using the RNeasy Mini kit (Qiagen) and 1 μ g RNA was reverse-transcribed using the iScript cDNA synthesis kit (Bio-Rad). The cDNAs were used as a template in qRT-PCR reactions containing the SYBR Green I fluorescent dye (Bio-Rad) and 10 pmol each forward and reverse primers (Supporting Information: Table S2). Reactions were performed in the LightCycler 480 Real-Time PCR system (Roche Diagnostics).

2.6 | Immunoblot analysis of TFIH subunits

Whole-cell lysates were prepared as previously described (Botta et al., 2002) and proteins were separated on 4%–12% gradient NuPAGE Bis-Tris gels (Thermo Fischer Scientific) and transferred onto nitrocellulose membranes (Protran, Whatman). Mouse antibodies against the TFIH subunits cdk7 (2F8), p44 (1H5), p62 (3C9), and XPD (2F6) were a gift from J.M. Egly (IGBMC) and were all diluted 1:2000. Mouse anti- γ -tubulin (T-6557, Sigma-Aldrich) was diluted 1:10,000. Chemiluminescent signals were detected using the ChemiDoc XRS system (Bio-Rad) and the density of the bands corresponding to the different proteins was quantified using the ImageJ 1.50i software (Schneider et al., 2012). The amount of each protein was normalized to the γ -tubulin amount and expressed as the mean value of the levels observed in two increasing concentrations of cell lysate. The relative levels of TFIH subunits in patient cells were expressed as percentages of the amounts present in the cells from the healthy donor C3PV analyzed in parallel. For TFIH quantification at 32 and 41°C, the levels of the different subunits were expressed as percentage of the values in C3PV fibroblasts grown at 37°C. Mean TFIH levels reported in Figures 2b and 3b were obtained by taking the average of the relative levels of the four analyzed subunits.

2.7 | Statistics

p Values were obtained by the unpaired two-tailed Student's *t*-test. Fisher *F*-ratio at a probability level (*p* value) of 0.05 was used to compare variances among the analyzed groups. Data are reported as mean \pm standard error of the mean (SEM). *p* Values <0.05 were considered significantly different.

3 | RESULTS

3.1 | Clinical history of the TTD cases showing temperature-sensitive symptoms

3.1.1 | TTD32PV

TTD32PV was an Italian male born in 2001 from unrelated parents, 2 years after a spontaneous abortion (Supporting Information: Figure S1). He was delivered by cesarean section performed at 33 gestational weeks because of mother pre-eclampsia and acute fetal distress. The mother presented gestational diabetes and thrombocytopenia. There was no notion of a collodion membrane and growth parameters were moderately reduced (Supporting Information: Table S3). Physiological jaundice (bilirubin 12.9 mg/dl) was observed on the third day after birth and was treated with phototherapy. In the first years of life, he showed borderline physical development and moderate delay in psychomotor development. Based on brittle hair, he was diagnosed with TTD at age 17 months. Parents reported temporary and recurrent loss of scalp hair during episodes of fever. Following an episode of gastroenteritis, at age 3 years and 6 months he was admitted to hospital for acute onset severe gait defect characterized by balance problems. He underwent physical therapy and in 2 months the gait defect gradually regressed, except for persistence of mild coordination defect. Since then, transient difficulty with walking and balance was observed together with hair loss during fever episodes. Brain magnetic resonance (MRI) revealed hypomyelination of the white matter. At age 4 years and 6 months, he showed delayed physical growth (Supporting Information: Table S3). The hair was wiry and thick and the skin dry and scaly. Neurological examination revealed slightly reduced motor coordination and reduced psychometric assessment (IQ 67 in the WPPSI scale). Further clinical signs were large ears and telecanthus. Brain MRI was repeated 1 year after the previous examination and T2-weighted magnetic resonance images confirmed hypomyelination of the white matter and dilated asymmetrical ventricles whereas computed tomography revealed no calcification. Brainstem-evoked potential reductions correlate with central myelinopathy. Motor and sensory nerve conduction velocities were within normal ranges, thus excluding involvement of peripheral nervous system myelin. No epileptic anomalies were shown by electroencephalogram. Blood tests revealed moderate microcytic anemia (hemoglobin [Hb] 10.6 g/dl [normal 11.5–15.5], hematocrit 33.2% [normal 40–54], mean corpuscular volume [MCV] 55 fl [normal 75–90], mean Hb content 17.6 pg [normal 27]). Urine tests and electrocardiogram were

normal. Unfortunately, clinicians lost contact with the family for follow-up.

3.1.2 | TTD34PV and TTD35PV

TTD34PV and TTD35PV are South Tyrol siblings born in 1996 and 2001, respectively (Supporting Information: Figure S2). The mother presented cystitis in the first trimester and pre-eclampsia at 34 gestational weeks (TTD34PV), uterine bleeding in the third month, and arterial hypertension from the fifth month (TTD35PV). At birth (39 gestational weeks for TTD34PV and 36 gestational weeks for TTD35PV), both siblings showed moderately reduced growth parameters (Supporting Information: Table S3) and the characteristic “collodion baby” appearance of the skin. TTD34PV was diagnosed with TTD at 6 years of age because of the presence of brittle, sparse, and dry hair with typical trichorrhexis nodosa-like fractures. Her scalp hair contained a low level of cysteine (9.01% [normal 18%]) and showed the typical “tiger tail” pattern under polarization microscopy. She also showed sun sensitivity. TTD35PV was diagnosed at 1 year and, in his first months of life, he suffered from bronchitis, pneumonia, and gastroenteritis. At 1 year and 7 months he had surgical correction (orchidopexy) of left cryptorchidism. In both siblings, neurological examination revealed normal muscle tone, no axial hypotonia, no spasticity, and no ataxia. TTD35PV presented fine motor disorders. They both showed ichthyotic skin, nail dysplasia, and astigmatism. TTD34PV was surgically treated for bilateral cataract at age 6 years whereas TTD35PV presents horizontal nystagmus. IQ scores for the TTD34PV patient were in the borderline intellectual disability and, although word comprehension was good, a mildly delayed speech development was reported. TTD35PV presented mild intellectual disability with reduced word comprehension and he started to attend primary school 1 year later compared to his classmates (at age 7). Hematological studies revealed microcythemia and slightly elevated levels of hemoglobin A2 (HbA2) in both siblings (TTD34PV at 12 years of age: Hb 13.2 g/dl [normal 12.0–18.0], MCV 68.7 fl [normal 80.0–99.0], MCH 3.3 pg [normal 27.0–31.0], MCHC 33.8% [normal 33.0–37.0], HbA2 6.0% [normal 1.8–3.6], HbF 0.8% [normal 0.1–1.8]; TTD35PV at 7 years of age: Hb 13.1 g/dl, MCV 69.2 fl, MCH 23.6 pg, MCHC 34.1%, HbA2 6.2%, HbF 0.7%). The presence of β -thalassemia trait, which was absent in both parents, represents a typical feature of TTD patients (Viprakasit et al., 2001).

At present, both siblings are employed in working activities outside the home. They show moderately reduced physical growth (Supporting Information: Table S3) and in TTD34PV further clinical signs are persistence of some deciduous teeth, slightly asymmetrical thorax, and pectus carinatum. The mother reports that in infancy the two siblings completely and reversibly lost their scalp hair during episodes of fever. From then on, they strictly control body temperature to avoid fever crisis.

3.1.3 | TTD37PV and TTD38PV

TTD37PV and TTD38PV are Canadian brothers born in 1988 and 1999, respectively, from unrelated parents of Scottish (father) and Welsh (mother) origin. TTD37PV has a healthy twin sister (Supporting Information: Figure S3) but no information is reported about their prenatal history except the fact the mother had a previous spontaneous abortion. At the time of diagnosis (20 years of age), TTD37PV showed yellow scales on scalp, brittle and coarse hair, thin and wavy nails, dry skin with freckles on cheeks, ichthyosis, and sun sensitivity. His physical growth was severely delayed (Supporting Information: Table S3) and he showed reduced muscle tone, mild axial hypotonia, cerebellar ataxia, contractures, gait abnormalities, and stooped appearance. He had congenital bilateral cataracts that were removed, multiple dental caries, osteosclerosis, seasonal and dust allergies. TTD37PV also presented chronic neutropenia and no anemia. A skeletal survey showed sclerosis and cranial thickening involving the axial skeleton and cranial vault with relative sparing of the skull base and appendicular skeleton. The acetabula were shallow and there was bilateral coxa valga with uncovering of the lateral femoral heads. He had bilateral hip surgery consisting of periacetabular osteotomy and reconstruction. He was noted to have dense and brittle bones during surgery. Bone abnormalities are in keeping with those recently reported in other TTD patients (DiGiovanna et al., 2022). Learning ability was moderately reduced but he could attend a special school program. At last examination (age 27), he presented upswing to anterior hairline and white scaly plaques all over the skin surface, in particular on flanks and groin region. He still suffered from hip pain. Brain imaging revealed hypomyelinating leukodystrophy.

His younger brother, TTD38PV, had similar features. The pregnancy with him was complicated by positive maternal serum screen with a risk of 1/8 for Down syndrome, and chorionic villus sampling was completed with a normal karyotype. At diagnosis (9 years of age), TTD38PV showed brittle, dry hair associated with ichthyotic skin. His physical growth was reduced (Supporting Information: Table S3) and hypomyelination of cerebral white matter was observed by brain imaging, even though it appeared less severe than in the brother. He also presented bilateral cataract but no surgery was required. At age 11 years he showed midcortical lens opacities and a central opacity with an abnormal red reflex bilaterally. He was last seen at age 16.5 years. He had simple ears, grooves on tongue, four missing teeth, sloping shoulders, and ichthyosis. Nails were short, broad, and brittle. The skeletal survey showed marked central osteosclerosis as well, involving the spine, pelvis, bilateral clavicles, posterior ribs, and cranial vault. He also showed mild weakness of proximal lower limbs. He has chronic neutropenia as well as increased HbA₂/total Hb ratio (0.040 [normal 0.018–0.032]) consistent with β -thalassemia trait (Viprakasit et al., 2001).

Both brothers reported that they have skin peeling and hair breaks when sick with fever.

3.2 | Cellular and molecular characterization of the temperature-sensitive TTD cases

3.2.1 | Response to UV light

About half of the reported TTD cases are PS-TTD and show an altered cellular response to UV light due to defective NER (Orioli & Stefanini, 2019). Thus, we measured the efficiency of NER activity on global genome by UDS in primary skin fibroblasts from the new TTD patients (TTD32PV, TTD34PV, TTD35PV, TTD37PV, and TTD38PV) upon UV irradiation.

We found drastically reduced UDS levels in all patient fibroblast strains (Figure 1a) implying that the temperature-sensitive TTD cases are NER-defective PS-TTD cases. Classical complementation studies in fusion tests assigned all patients to the XP-D group (Figure 1b), pointing to defects in the *ERCC2* gene that encodes the XPD subunit of TFIIH.

3.2.2 | Novel *ERCC2* variants

ERCC2 mutant alleles and their inheritance were investigated by Sanger sequencing in patient and parent cells (Supporting Information: Figures S1–S3). We found that TTD32PV carries the c.2074A>G variant resulting in the p.Lys692Glu substitution in the paternal *ERCC2* allele and the c.1846C>T change leading to p.Arg616Trp in the maternal allele (Figure 1c and Supporting Information: Figure S1). So far, the p.Lys692Glu change has never been associated with a pathological condition whereas p.Arg616Trp has been already associated with both TTD and XP phenotypes and considered a “null allele” (Taylor et al., 1997). Mutations on both *ERCC2*/*XPD* alleles may however contribute to the thermo-sensitive TTD clinical manifestations as already shown for the broad range of and severity of clinical features in XPD-defective XP patients (Ueda et al., 2009).

The siblings TTD34-35PV inherited from the father the c.335G>A mutation that results in the p.Arg112His change, a frequently found alteration in PS-TTD cases (Orioli & Stefanini, 2019). A novel c.2191-1G>A splice variant was inherited from the mother. PCR amplification and sequencing of *ERCC2* cDNA demonstrates that the splice variant partially affects the recognition of intron 22 acceptor splice site generating both a mutant transcript that retains intron 22 (c.2190_2191ins intron 22) and a normally spliced transcript (Supporting Information: Figure S2). Allele-specific qRT-PCR assays showed that mutant and normal transcripts are produced with the same efficiency each accounting for about 30% of the total *ERCC2* transcripts. Insertion of intron 22 alters the reading frame and is predicted to result in a frameshift from position 731 that runs into a stop codon 100 amino acids ahead, thus producing an 830 amino acid long protein (p.Glu731Valfs*100) that is longer than normal XPD (760 amino acids) (Figure 1c).

Two novel *ERCC2* variants were finally identified in the TTD37-38PV brothers. The paternal allele carries the c.1963G>T missense variant resulting in p.Asp655Tyr whereas the maternal allele carries

the c.1867dupG duplicating insertion predicted to result in the frameshift p.Val623Glyfs*26 (Figure 1c and Supporting Information: Figure S3). However, the insertion could not be identified on sequencing traces of PCR-amplified *ERCC2* cDNA fragments (Supporting Information: Figure S3) indicating poor expression. Investigations with allele-specific qRT-PCR assays confirmed that, in patient cells, c.1867dupG is only found in 10% of the total *ERCC2* transcripts whereas the remaining 90% contain the c.1963G>T change.

In conclusion, all new cases are compound heterozygotes carrying novel variants on at least one mutant *ERCC2* allele. The new variants are all extremely rare in the human population. In particular, c.2074A>G (TTD32PV), c.2191-1G>A (TTD34-35PV), and c.1963G>T (TTD37-38PV) are not found in the aggregate 150,000 human genomes available from the Genome Aggregation Database (gnomAD v2.1.1). The c.1867dupG change (TTD37-38PV) is present in gnomAD with low frequency (0,00005699) and no homozygosity has been reported. CADD_phred v 1.5 scores greater than 20 (29.6 for p.Lys692Glu resulting from c.2074A>G and 24.5 for p.Asp655Tyr resulting from c.1963G>T) support damaging effect for the missense changes.

3.2.3 | Cellular amount of the mutant TFIIH complexes

PS-TTD-related XPD alterations typically result in reduced overall cellular content of TFIIH complex (Botta et al., 2002; Vermeulen et al., 2000, 2001). Consistently, immunoblot analysis of primary fibroblast lysates demonstrated a relevant decrease in the steady-state levels of XPD, p62, p44, and cdk7 subunits of TFIIH in all new patients compared to the healthy donor C3PV (Figure 1d). In fibroblasts from TTD32PV and TTD37-38PV siblings, the residual amounts of the four TFIIH subunits correspond to about 40%–50% of those of control. Differently, in TTD34-35PV fibroblasts, the levels of p62, p44, and cdk7 are reduced to about 60% of normal whereas a more drastic reduction to about 30%–35% is observed in XPD level (Figure 1d). This is likely due to the fact that the predicted mutant XPD protein p.Glu731Valfs*100 may not be detected by the XPD antibody that is directed against the 728–760 epitope, largely modified by the frameshift. Considering the protein amount of the other TFIIH subunits, we can assert that all the newly identified XPD alterations cause TFIIH instability, in agreement with previous findings.

3.3 | Functional studies in patient primary fibroblasts

3.3.1 | Temperature effect on the mutant TFIIH complexes

To verify whether temperature impacts the stability and functionality of TFIIH complexes containing the newly identified mutant XPD

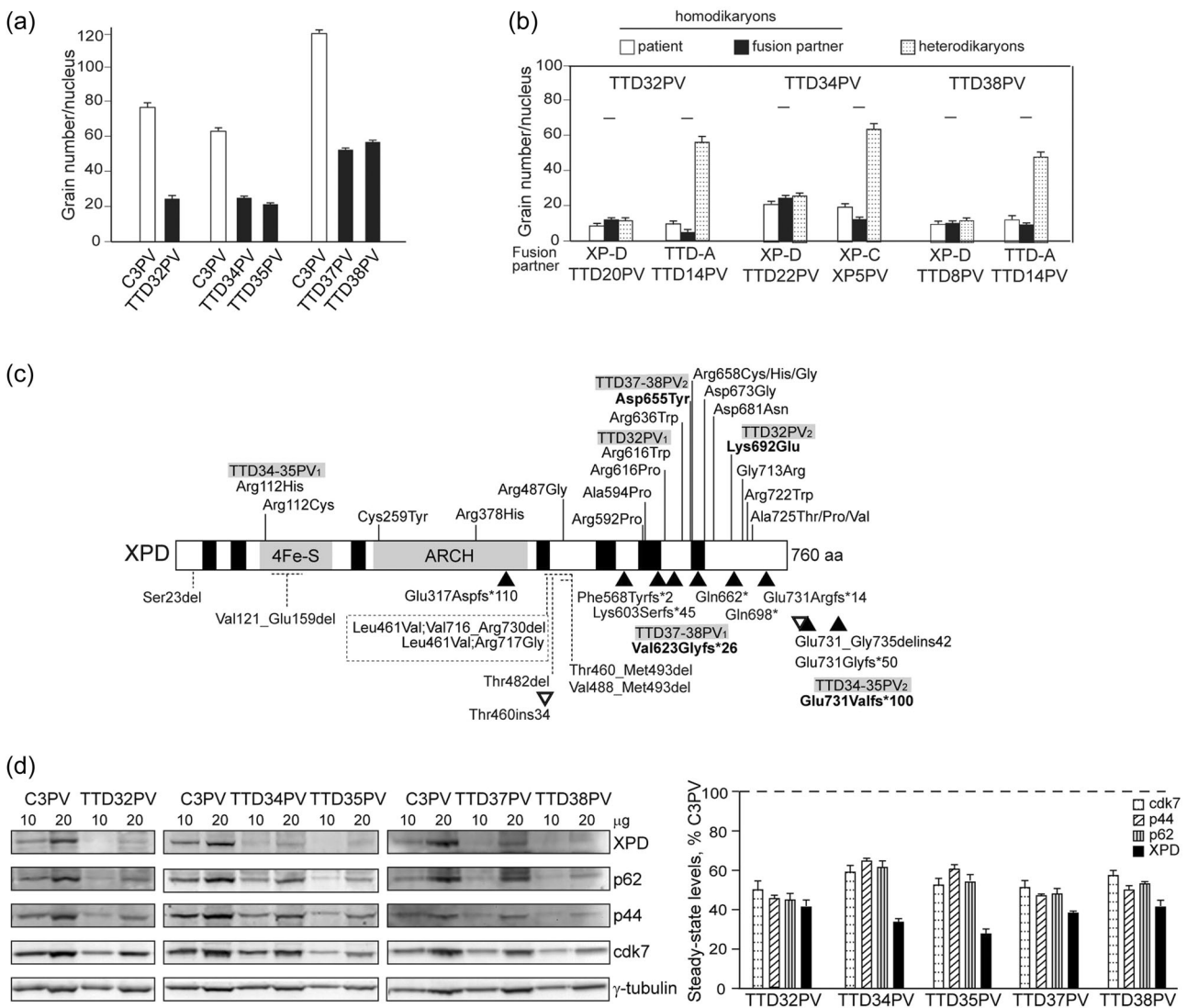


FIGURE 1 Cellular and molecular characterization of the TTD cases TTD32PV, TTD34PV, TTD35PV, TTD37PV, and TTD38PV. (a) UDS levels in fibroblasts from the patients and the healthy donor C3PV following irradiation with 20 J/m² UV-C. Cells were pulse-labeled for 3 h with ³H-thymidine before processing. Reported values represent the mean \pm SEM ($n = 50$). (b) Complementation analysis of the UDS defect in heterodikaryons obtained by fusion of TTD32PV, TTD34PV, and TTD38PV fibroblasts with reference strains. The mean number of autoradiographic grains per nucleus in homodikaryons (patients, white columns; fusion partners, black columns) and in heterodikaryons (dotted columns) is shown. Reported values represent the mean \pm SEM ($n = 25$). The horizontal lines indicate the grain number per nucleus in C3PV fibroblasts analyzed in parallel. (c) Aminoacid changes in the XPD protein from mutations described in PS-TTD patients. The diagram shows the XPD protein with the helicase motifs in black; 4Fe-S and ARCH domains are in gray. Missense changes are indicated by solid lines, truncations are indicated by triangles whereas in-frame deletions are represented by dotted horizontal lines and insertions or deletion/insertions are indicated by white triangles. The complex allele carrying two combined alterations and expressing both p.[Leu461Val; Val716_Arg730del] and p.[Leu461Val; Arg717Gly] (Horibata et al., 2015) is shown boxed. The codes of the new patients are reported over the corresponding alterations; numbers 1 and 2 denote the different alleles; novel alterations are in bold. Mutation nomenclature follows the format indicated at www.hgvs.org/mutnomen. Protein sequence refers to GenBank NP_000391.1. (d) Immunoblots of fibroblast lysates. Ten and 20 μ g of each lysate were separated on gels and blots were probed with antibodies against the TFIIH subunits XPD, p62, p44, and cdk7, and the loading control γ -tubulin (left). TFIIH subunit levels were normalized to γ -tubulin and expressed as percentages of the values in C3PV fibroblasts (right). Reported values represent the mean \pm SEM of three independent experiments. PS-TTD, photosensitive form of TTD; RS, RNA synthesis rate; TTD, trichothiodystrophy; UDS, unscheduled DNA synthesis.

proteins, we monitored TFIIH subunit levels and complex activities in patient cells following shift from standard 37°C to either lower (32°C) or higher (41°C) temperature (Figure 2a). Investigations were carried out on primary fibroblasts from patients TTD32PV, TTD34PV, and TTD38PV representative of the new XPD alterations. Controls

included fibroblasts from (i) the healthy donor C3PV, (ii) TTD12PV, TTD23PV, and TTD8PV patients representative of the most frequent alterations in PS-TTD/XP-D cases (Supporting Information: Table S1) but with no evidence of fever-dependent symptoms (Battistella & Peserico, 1996 [TTD8PV], Supplemental Note [TTD12PV and

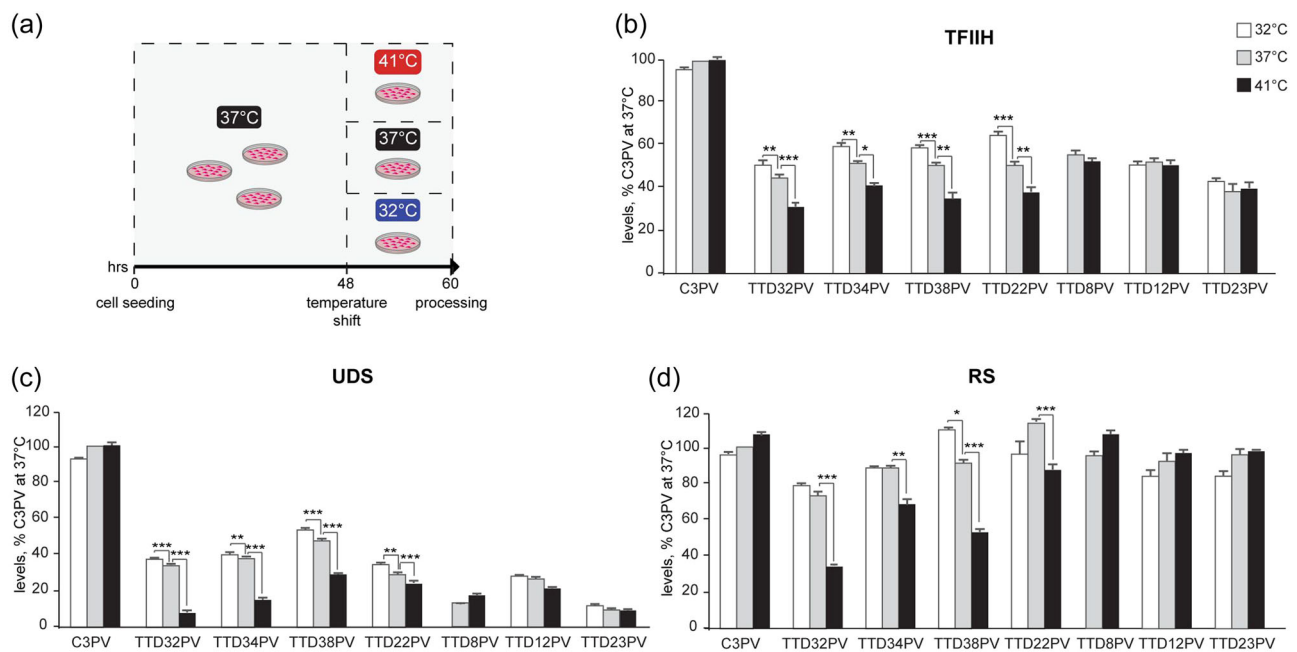


FIGURE 2 Effect of temperature on TFIIH stability and activity. (a) Experimental scheme. Parallel cultures of primary fibroblasts were grown at 37°C for 48 h and then either maintained at 37°C or moved to 32 or 41°C for additional 12 h before processing. (b–d) TFIIH (b), UDS (c), and RS (d) levels in primary fibroblasts from the thermo-sensitive patients TTD32PV, TTD34PV, TTD38PV, and TTD22PV, the non-thermo-sensitive patients TTD8PV, TTD12PV, and TTD23PV and the healthy donor C3PV. (b) Immunoblots of cell lysates were probed with antibodies against the TFIIH subunits XPD, p62, p44, and cdk7, and the loading control γ -tubulin. The levels of the different TFIIH subunits were normalized to γ -tubulin and expressed as the percentage of the values in C3PV fibroblasts grown at 37°C. TFIIH levels were then expressed as mean levels of the analyzed subunits. (c) UDS was evaluated following a UV-C dose of 20 J/m². For each sample the mean number of autoradiographic grains/nucleus was calculated in at least 25 cells and then UDS levels were expressed as the percentage of the values in C3PV fibroblasts grown at 37°C. (d) RS was evaluated following a 1 h pulse with ³H-uridine. For each sample the mean number of autoradiographic grains/nucleus was calculated in at least 25 cells and then RS levels were expressed as the percentage of the values in C3PV fibroblasts grown at 37°C. All reported values represent the mean \pm SEM of at least three independent experiments. * $p < .05$, ** $p < .01$, *** $p < .001$ (Student's *t*-test).

TTD23PV)), and (iii) TTD22PV patient who carries a mutation that results in multiple out of frame XPD mutant proteins including the p.Glu731Valfs*100 protein (Supporting Information: Table S1), also predicted from a different mutation in the siblings TTD34–35PV.

Upon 12-h incubation at either 32 or 41°C, TFIIH cell content was evaluated by immunoblot analysis using antibodies directed against the XPD, p62, p44, and cdk7 subunits (Supporting Information: Figure S4). In parallel, TFIIH functionality in NER was assessed by UDS assays after exposing the fibroblasts to UV irradiation whereas TFIIH activity in transcription was evaluated by measuring the overall RS. Notably, temperature shifts yielded a clear-cut distinction between non-thermo-sensitive and thermo-sensitive cells (Figure 2b–d). TFIIH subunit amounts, UDS levels, and RS rates at 32°C and/or 41°C remained similar to those observed at 37°C in fibroblasts from C3PV as well as in fibroblasts from TTD12PV, TTD23PV, and TTD8PV patients. In contrast, temperature-related variations were observed in TTD32PV, TTD34PV, TTD38PV, and TTD22PV fibroblasts (Figure 2b). In detail, temperature increment to 41°C produced a significant drop in the amounts of all analyzed TFIIH subunits (to 30%–40% of C3PV) whereas temperature decrement to 32°C significantly increased their residual levels (from 40%–50% to 60%–65% of C3PV). These findings demonstrate that temperature

variations impact on TFIIH cellular content in a mutation-dependent manner. Hence, they allow to define TTD22PV as a thermo-sensitive case although no relevant clinical information is available (Botta et al., 2009). Thermo-instability directly affects the XPD protein since temperature has no significant effect on *ERCC2* transcript amounts (Supporting Information: Figure S5).

Concerning functionality, the increment of TFIIH amount at 32°C was paralleled by a slight increase of UDS levels (from 30%–35% to 40% of C3PV in TTD32PV, TTD34PV, and TTD22PV and from 50% to 55% in TTD38PV, Figure 2c) and normal RS levels (Figure 2d). In contrast, the decrement of TFIIH concentration at 41°C was paralleled by a strong reduction of UDS levels (to 10%–30% of C3PV, Figure 2c) and a drastic reduction of RS rates (to 20%–70% of C3PV, Figure 2d). Therefore, TFIIH thermo-instability finally results in temperature-dependent deficiencies in NER and transcription.

3.3.2 | Glycerol effect on the mutant TFIIH complexes

Lowering the growth culture temperature of thermo-sensitive PS-TTD/XP-D fibroblasts to 32°C results in increased cellular

content of the mutated XPD proteins. A reduced temperature is known to promote the process of protein folding in in vitro-cultured cells (Ulloa-Aguirre et al., 2004), suggesting temperature-dependent mutant XPD misfolding. To clarify the nature of XPD alterations we explored the effect of glycerol, a small polyol frequently used as a chemical chaperone able to enhance the in vivo folding pathways of proteins (Brown et al., 1997). Parallel samples of fibroblasts were incubated for 12 h in culture medium supplemented or not with glycerol and, subsequently, the amount of XPD and other TFIIH subunits as well as the UDS and RS levels were evaluated (Figure 3a). Of note, we found that glycerol supplementation significantly increased TFIIH amount in TTD32PV, TTD34PV, TTD38PV, and TTD22PV fibroblasts incubated at 41°C, approaching the levels detected in cells grown at 37°C (Supporting Information: Figure S6 and Figure 3b). No effect of glycerol was instead observed in cells from the non-thermosensitive cases TTD8PV, TTD12PV, and

TTD23PV (Supporting Information: Figure S6). TFIIH increment was paralleled by significantly higher UDS and RS levels (Figure 3c,d). Thus, glycerol can prevent the drastic quantitative drop of TFIIH subunits and the consequent aggravation of TFIIH complex dysfunction observed at high temperatures in thermo-sensitive patient cells. This indicates that thermo-sensitivity of mutant XPD subunits can be at least partially rescued by a molecular chaperone promoting protein folding.

4 | DISCUSSION

We have identified four novel alterations in the XPD subunit of the DNA repair/transcription factor TFIIH (namely, p.Asp655Tyr, p.Lys692Glu, p.Val623Glyfs*26, and p.Glu731Valfs*100) in three families with PS-TTD cases characterized by episodic and reversible

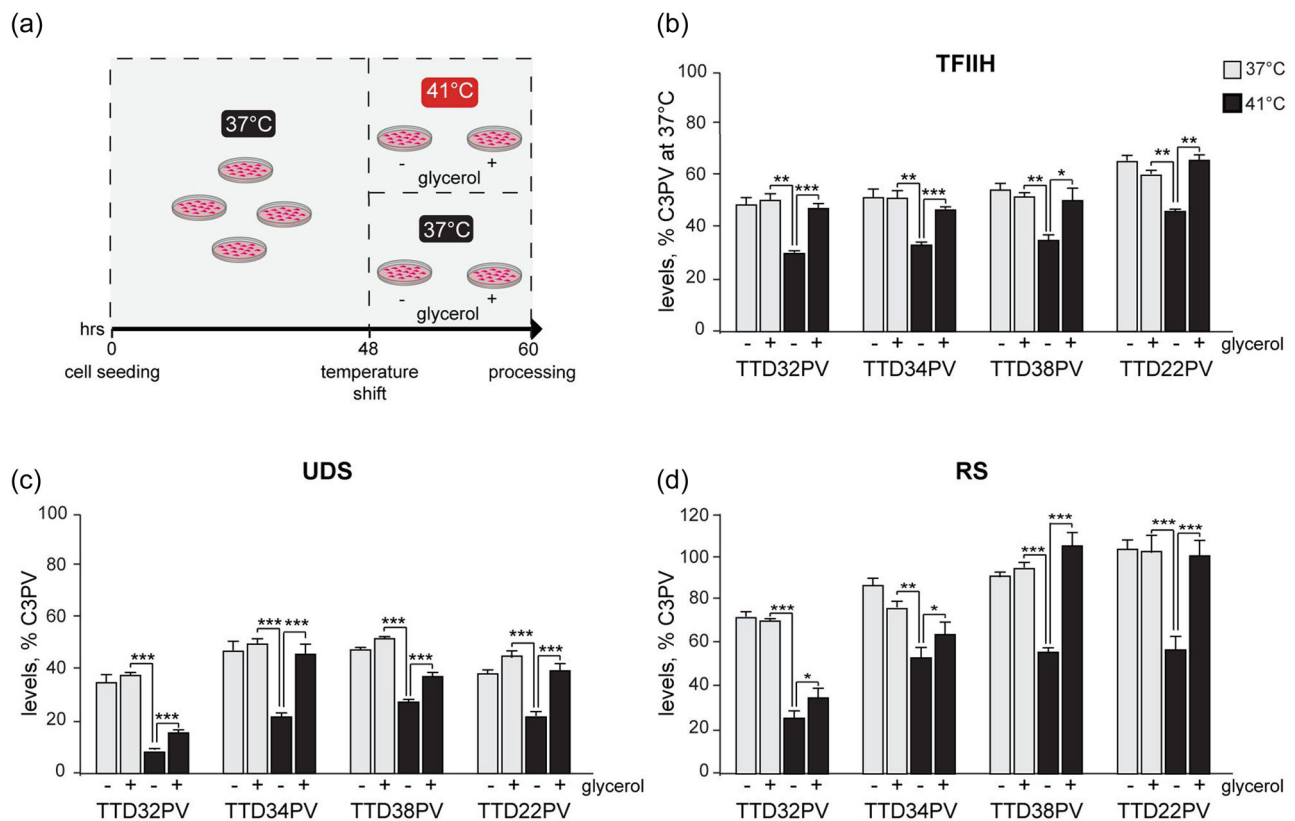


FIGURE 3 Effect of glycerol on TFIIH stability and activity. (a) Experimental scheme. Parallel cultures of primary fibroblasts were grown at 37°C for 48 h and then incubated either at 37 or 41°C in the presence or absence of 0.66 M glycerol for further 12 h before processing. (b–d) TFIIH (b), UDS (c), and RS (d) levels in primary fibroblasts from TTD32PV, TTD34PV, TTD38PV, and TTD22PV and the healthy donor C3PV. (b) Immunoblots of cell lysates were probed with antibodies against the TFIIH subunits XPD, p62, p44, and cdk7, and the loading control γ -tubulin. The levels of the different TFIIH subunits were normalized to γ -tubulin and expressed as the percentage of the values in the corresponding C3PV samples. TFIIH levels were then expressed as mean levels of the analyzed subunits. (c) UDS was evaluated following a UV-C dose of 20 J/m². For each sample the mean number of autoradiographic grains/nucleus was calculated in at least 25 cells and then UDS levels were expressed as the percentage of the values in the corresponding C3PV samples. (d) RS was evaluated following a 1 h pulse with ³H-uridine. For each sample the mean number of autoradiographic grains/nucleus was calculated in at least 25 cells and then RS levels were expressed as the percentage of the values in the corresponding C3PV samples. All reported values represent the mean \pm SEM of at least three independent experiments. * $p < .05$, ** $p < .01$, *** $p < .001$ (Student's *t*-test). RS, RNA synthesis rate; TFIIH, transcription factor IIH; UDS, unscheduled DNA synthesis.

aggravation of symptoms concurrently with febrile episodes. Similar fever-related severity of clinical features was earlier reported in four patients, three of whom were consanguineous (Hansen et al., 1993; Kleijer et al., 1994). The previously described affected individuals all carried an identical mutation leading to the amino acid substitution p.Arg658Cys in XPD (Vermeulen et al., 2001). Our study further adds to thermo-sensitive clinical presentations in PS-TTD showing that this peculiar phenotype may be related to different sets of XPD alterations.

Considering all XPD mutations so far related to the thermo-sensitive PS-TTD phenotype (this paper and Vermeulen et al., 2001), we can state that they map to the C-terminal third of the XPD protein, as it is for the majority of disease causing changes in XPD (Figure 1c). The high-resolution cryo-electron microscopy structures of the entire human TFIIH (Greber et al., 2019; Yan et al., 2019) highlighted that PS-TTD mutations are generally located in alpha-helix structures at the periphery of XPD and are predicted to affect XPD interactions within the complex by disrupting protein–protein interfaces, either directly or through breaks in helices at interfaces. Thus, PS-TTD mutations weaken the assembly of TFIIH subunits, as demonstrated by the reduced levels of TFIIH complex typically found in all PS-TTD cells (Botta et al., 2002; Vermeulen et al., 2000, 2001). In fibroblasts from the newly identified thermo-sensitive cases, the

degree of TFIIH reduction is further aggravated upon incubation at 41°C, as previously reported for cells carrying the XPD variant p.Arg658Cys (Vermeulen et al., 2001). Of note, among all the mutations related to thermo-sensitivity, missense changes affect the residues Asp655, Arg658, and Lys692 that are in close proximity in the 3D structure of XPD (Figure 4a), suggesting a temperature-sensitive spatial peptide cluster. Investigations in thermo-sensitive patient cells also demonstrated that the reduced cellular content of mutant XPD proteins and, by consequence, of other TFIIH subunits could be partially rescued by dropping culture temperature to 32°C or by exposing cells to the molecular chaperone glycerol (Figures 2 and 3). Both treatments favor the protein folding process, supporting the notion that XPD thermo-sensitive alterations might result in temperature-dependent misfolding. Furthermore, by the ESBRI online tool (<http://bioinformatica.isa.cnr.it/ESBRI/>, Costantini et al., 2008) residues Asp655, Arg658, and Lys692 are predicted to form networks of salt bridges (Supporting Information: Table S4). Salt bridges in proteins are formed between oppositely charged residues that are sufficiently close to each other to experience electrostatic attraction. They play an important role in maintaining protein structure and may contribute to protein stability at high temperatures (Bosshard et al., 2004; Folch et al., 2008). Among the 34 salt bridges predicted in silico in XPD, several involve the thermo-sensitive

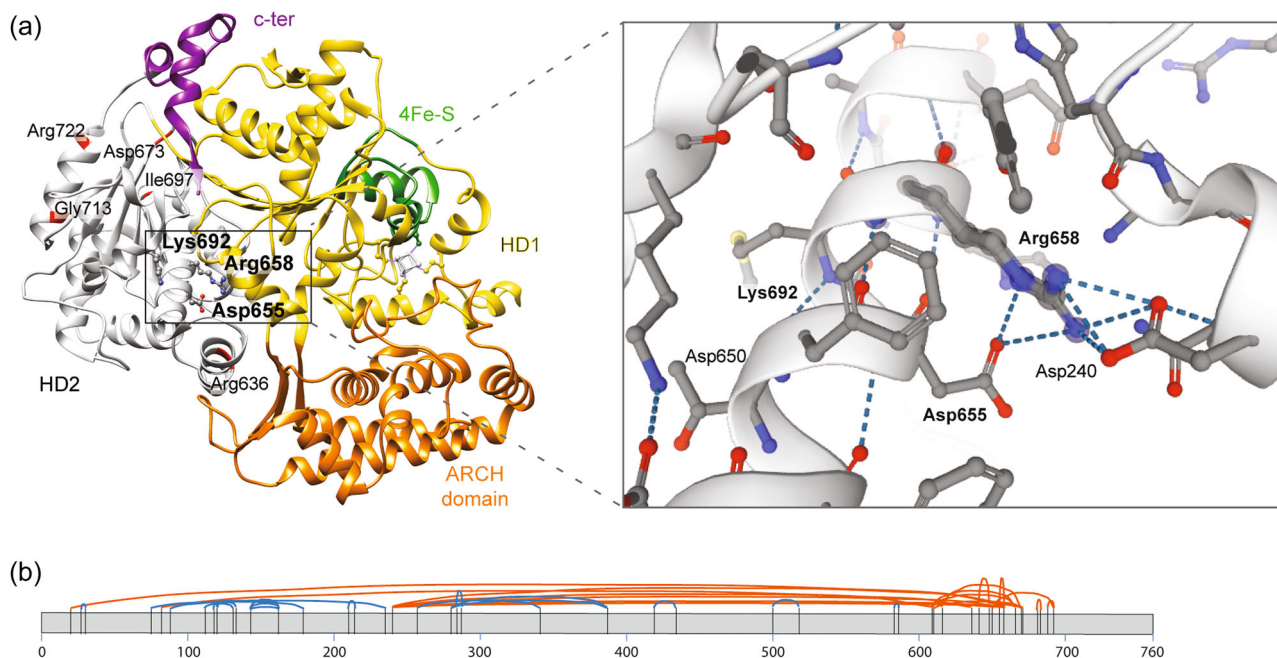


FIGURE 4 Insights in the XPD protein. (a) 3-D structure of the human XPD protein (PDB 6nmi, chain B; molecular graphic performed with UCSF Chimera (<https://www.cgl.ucsf.edu/chimera/> (Pettersen et al., 2004)). The different domains are shown in colors; the two Rec-A like helicase motor domains HD1 and HD2 in yellow and white, respectively; the 4Fe4S domain in green; the ARCH domain in orange; and the C-terminal domain in dark magenta. Residues affected by thermo-sensitive missense mutations are boxed. On the right, visualization of salt bridges involving these residues (ProteinTools, <https://proteintools.uni-bayreuth.de/salt/>; Ferruz et al., 2021). The software automatically computes the fraction of charged residues (FCR) and the kappa value (κ) according to CIDER (Classification of Intrinsically Disordered Ensemble Regions, <http://pappulab.wustl.edu/CIDER/>) and renders salt bridges in proteins with a distance cut-off between residues participating in salt bridges below 4 Å. (b) Overall distribution of salt bridges in the XPD sequence as predicted by ESBRI (<http://bioinformatica.isa.cnr.it/ESBRI/>). Atomic coordinates of the 6nmi PDB structure were provided and analyzed for chain B, with a 4.0 Å distance between charged residues. Salt bridges involving residues from position 609 to 692 are in orange.

residues. In particular, a salt bridge directly links residues Arg658 and Asp655. One additional salt bridge links Asp655 and His659 whereas four are formed between Arg658 and Asp240. In addition, two salt bridges link Lys692 to Asp650 and Asp688 (Figure 4a, right panel, Supporting Information: Table S4). Considering that proteins fold into their native structures by an interplay of various noncovalent interactions (which include ionic interactions and salt bridges), we are tempted to speculate that mutations at residues Asp655, Arg658, and Lys692, may result in thermo-sensitive forms of XPD protein by perturbing the balance between salt bridges formation and folding. Although our observation remains speculative, it is worth noticing that a large number of XPD salt bridges (18 out of 34) involve residues mapping from position 609 to 692 (Figure 4b), likely indicating a protein region relevant for temperature sensitivity.

Worsening of mutant TFIH instability by high temperature causes an aggravation of TFIH functional deficiencies (Figure 2). On the other hand, partial rescue of TFIH cellular amount by temperature reduction improves the functional efficiency of the complex (Figure 2). These findings highlight how variations in the cellular concentration of mutated TFIH impact on its functionality and provide evidence on how both quantitative and qualitative TFIH alterations contribute to the PS-TTD phenotype. Furthermore, our findings provide a rationale for the TTD thermo-sensitive clinical features. It is likely that when a patient with a thermo-sensitive XPD mutation has fever, the stability, and functionality of TFIH decrease leading to aggravation of symptoms. This highlights the relevance of preventing fever crises which exacerbate disease manifestations. Intriguingly, in the thermo-sensitive patients only specific clinical features show fever-dependent aggravation, namely hair fragility, gait defects, and skin alterations. It has been proposed that the diverse clinical manifestations of PS-TTD reflect subtle defects in RNAPII transcription, which, though compatible with life, impair specific gene functions that require high levels of transcription (de Boer et al., 1998). In most cells, continuous de novo synthesis of the complex may, at least in part, compensate for TFIH instability. However, in terminally differentiated tissues specific sets of genes are transcribed at very high rate and unstable TFIH complexes may be depleted before terminal differentiation is complete. This phenomenon becomes more pronounced in TTD patients carrying thermo-sensitive alterations, when high body temperature further destabilizes TFIH.

In conclusion, we report novel thermo-labile variants of the XPD subunit of the TFIH complex that might reflect protein folding alterations. By functional investigations in PS-TTD patient cells carrying the novel XPD variants, we demonstrate the direct relationship of quantitative variations in TFIH cellular content and its functional activities. These observations in XPD-defective patients, strongly support the link between TFIH amount and PS-TTD symptoms.

ACKNOWLEDGMENTS

We are grateful to the families of patients for participation in this study. The work was supported by Associazione Italiana Ricerca sul Cancro (Id. 21737) to Donata Orioli.

CONFLICT OF INTEREST

The authors declare no conflict of interest.

ORCID

Elena Botta  <http://orcid.org/0000-0003-2060-0110>

REFERENCES

- Arseni, L., Lanzafame, M., Compe, E., Fortugno, P., Afonso-Barroso, A., Peverali, F. A., Lehmann, A. R., Zambruno, G., Egly, J. M., Stefanini, M., & Orioli, D. (2015). TFIH-dependent MMP-1 overexpression in trichothiodystrophy leads to extracellular matrix alterations in patient skin. *Proceedings of the National Academy of Sciences USA*, *112*, 1499–1504. <https://doi.org/10.1073/pnas.1416181112>
- Battistella, P. A., & Peserico, A. (1996). Central nervous system dysmyelination in PIBI(D)S syndrome: A further case. *Child's Nervous System*, *12*, 110–113. <https://doi.org/10.1007/BF00819509>
- de Boer, J., de Wit, J., van Steeg, H., Berg, R. J. W., Morreau, H., Visser, P., Lehmann, A. R., Duran, M., Hoeijmakers, J. H. J., & Weeda, G. (1998). A mouse model for the basal transcription/DNA repair syndrome trichothiodystrophy. *Molecular Cell*, *1*, 981–990. [https://doi.org/10.1016/s1097-2765\(00\)80098-2](https://doi.org/10.1016/s1097-2765(00)80098-2)
- Bosshard, H. R., Marti, D. N., & Jelesarov, I. (2004). Protein stabilization by salt bridges: Concepts, experimental approaches and clarification of some misunderstandings. *Journal of Molecular Recognition*, *17*, 1–16. <https://doi.org/10.1002/jmr.657>
- Botta, E., Nardo, T., Lehmann, A. R., Egly, J. M., Pedrini, A. M., & Stefanini, M. (2002). Reduced level of the repair/transcription factor TFIH in trichothiodystrophy. *Human Molecular Genetics*, *11*, 2919–2928. <https://doi.org/10.1093/hmg/11.23.2919>
- Botta, E., Nardo, T., Broughton, B. C., Marinoni, S., Lehmann, A. R., & Stefanini, M. (1998). Analysis of mutations in the XPD gene in Italian patients with trichothiodystrophy: Site of mutation correlates with repair deficiency, but gene dosage appears to determine clinical severity. *The American Journal of Human Genetics*, *63*, 1036–1048. <https://doi.org/10.1086/302063>
- Botta, E., Nardo, T., Orioli, D., Guglielmino, R., Ricotti, R., Bondanza, S., Benedicenti, F., Zambruno, G., & Stefanini, M. (2009). Genotype-phenotype relationships in trichothiodystrophy patients with novel splicing mutations in the XPD gene. *Human Mutation*, *30*, 438–445. <https://doi.org/10.1002/humu.20912>
- Brown, C. R., HongBrown, L. Q., & Welch, W. J. (1997). Correcting temperature-sensitive protein folding defects. *Journal of Clinical Investigation*, *99*, 1432–1444. <https://doi.org/10.1172/JCI119302>
- Chavanne, F., Broughton, B. C., Pietra, D., Nardo, T., Browitt, A., Lehmann, A. R., & Stefanini, M. (2000). Mutations in the XPC gene in families with xeroderma pigmentosum and consequences at the cell, protein, and transcript levels. *Cancer Research*, *60*, 1974–1982.
- Compe, E., Drané, P., Laurent, C., Diderich, K., Braun, C., Hoeijmakers, J. H. J., & Egly, J. M. (2005). Dysregulation of the peroxisome proliferator-activated receptor target genes by XPD mutations. *Molecular and Cellular Biology*, *25*, 6065–6076. <https://doi.org/10.1128/MCB.25.14.6065-6076.2005>
- Compe, E., & Egly, J. M. (2016). Nucleotide excision repair and transcriptional regulation: TFIH and beyond. *Annual Review of Biochemistry*, *85*, 265–290. <https://doi.org/10.1146/annurev-biochem-060815-014857>
- Compe, E., Malerba, M., Soler, L., Marescaux, J., Borrelli, E., & Egly, J. M. (2007). Neurological defects in trichothiodystrophy reveal a coactivator function of TFIH. *Nature Neuroscience*, *10*, 1414–1422. <https://doi.org/10.1038/nn1990>
- Costantini, S., Colonna, G., & Facchiano, A. M. (2008). ESBR1: A web server for evaluating salt bridges in proteins. *Bioinformatics*, *3*, 137–138. <https://doi.org/10.6026/97320630003137>

- DiGiovanna, J. J., Randall, G., Edelman, A., Allawh, R., Xiong, M., Tamura, D., Khan, S. G., Rizza, E. R. H., Reynolds, J. C., Paul, S. M., Hill, S. C., & Kraemer, K. H. (2022). Debilitating hip degeneration in trichothiodystrophy: Association with ERCC2 / XPD mutations, osteosclerosis, osteopenia, coxa valgus, contractures, and osteonecrosis. *American Journal of Medical Genetics Part A. Portico*. <https://doi.org/10.1002/ajmg.a.62962>
- Dubaele, S., De Santis, L. P., Bienstock, R. J., Keriell, A., Stefanini, M., Van Houten, B., & Egly, J. M. (2003). Basal transcription defect discriminates between xeroderma pigmentosum and trichothiodystrophy in XPD patients. *Molecular Cell*, 11, 1635–1646. [https://doi.org/10.1016/s1097-2765\(03\)00182-5](https://doi.org/10.1016/s1097-2765(03)00182-5)
- Faghri, S., Tamura, D., Kraemer, K. H., & DiGiovanna, J. J. (2008). Trichothiodystrophy: A systematic review of 112 published cases characterises a wide spectrum of clinical manifestations. *Journal of Medical Genetics*, 45, 609–621. <https://doi.org/10.1136/jmg.2008.058743>
- Ferri, D., Orioli, D., & Botta, E. (2020). Heterogeneity and overlaps in nucleotide excision repair disorders. *Clinical Genetics*, 97, 12–24. <https://doi.org/10.1111/cge.13545>
- Ferruz, N., Schmidt, S., & Höcker, B. (2021). ProteinTools: A toolkit to analyze protein structures. *Nucleic Acids Research*, 49, W559–W566. <https://doi.org/10.1093/nar/gkab375>
- Folch, B., Rooman, M., & Dehouck, Y. (2008). Thermostability of salt bridges versus hydrophobic interactions in proteins probed by statistical potentials. *Journal of Chemical Information and Modeling*, 48, 119–127. <https://doi.org/10.1021/ci700237g>
- Giglia-Mari, G., Coin, F., Ranish, J. A., Hoogstraten, D., Theil, A., Wijgers, N., Jaspers, N. G. J., Raams, A., Argentini, M., van der Spek, P. J., Botta, E., Stefanini, M., Egly, J. M., Aebersold, R., Hoeijmakers, J. H. J., & Vermeulen, W. (2004). A new, tenth subunit of TFIIH is responsible for the DNA repair syndrome trichothiodystrophy group A. *Nature Genetics*, 36, 714–719. <https://doi.org/10.1038/ng1387>
- Greber, B. J., Toso, D. B., Fang, J., & Nogales, E. (2019). The complete structure of the human TFIIH core complex. *eLife*, 8, e4477. <https://doi.org/10.7554/eLife.44771>
- Hansen, L. K., Wulff, K., & Brandrup, F. (1993). [Trichothiodystrophy. Hair examination as a diagnostic tool]. *Ugeskrift For Laeger*, 155, 1949–1952.
- Horibata, K., Kono, S., Ishigami, C., Zhang, X., Aizawa, M., Kako, Y., Ishii, T., Kosaki, R., Saijo, M., & Tanaka, K. (2015). Constructive rescue of TFIIH instability by an alternative isoform of XPD derived from a mutated XPD allele in mild but not severe XP-D/CS. *Journal of Human Genetics*, 60, 259–265. <https://doi.org/10.1038/jhg.2015.18>
- Kleijer, W. J., Beemer, F. A., & Boom, B. W. (1994). Intermittent hair loss in a child with PIBI(D)S syndrome and trichothiodystrophy with defective DNA repair-xeroderma pigmentosum group D. *American Journal of Medical Genetics*, 52, 227–230. <https://doi.org/10.1002/ajmg.1320520220>
- Kuschal, C., Botta, E., Orioli, D., DiGiovanna, J. J., Seneca, S., Keymolen, K., Tamura, D., Heller, E., Khan, S. G., Caligiuri, G., Lanzafame, M., Nardo, T., Ricotti, R., Peverali, F. A., Stephens, R., Zhao, Y., Lehmann, A. R., Baranello, L., Levens, D., ... Stefanini, M. (2016). GTF2E2 mutations destabilize the general transcription factor complex TFIIIE in individuals with DNA repair-proficient trichothiodystrophy. *The American Journal of Human Genetics*, 98, 627–642. <https://doi.org/10.1016/j.ajhg.2016.02.008>
- Lombardi, A., Arseni, L., Carriero, R., Compe, E., Botta, E., Ferri, D., Uggè, M., Biamonti, G., Peverali, F. A., Bione, S., & Orioli, D. (2021). Reduced levels of prostaglandin I2 synthase: A distinctive feature of the cancer-free trichothiodystrophy. *Proceedings of the National Academy of Sciences*, 118, e2024502118. <https://doi.org/10.1073/pnas.2024502118>
- Orioli, D., Compe, E., Nardo, T., Mura, M., Giraudon, C., Botta, E., Arrigoni, L., Peverali, F. A., Egly, J. M., & Stefanini, M. (2013). XPD mutations in trichothiodystrophy hamper collagen VI expression and reveal a role of TFIIH in transcription derepression. *Human Molecular Genetics*, 22, 1061–1073. <https://doi.org/10.1093/hmg/dd508>
- Orioli, D., & Stefanini, M. (2019). Trichothiodystrophy. In C. Nishigori & K. Sugawara (Eds.), *DNA repair disorders-clinical and molecular aspects*. Springer-Japan.
- Pettersen, E. F., Goddard, T. D., Huang, C. C., Couch, G. S., Greenblatt, D. M., Meng, E. C., & Ferrin, T. E. (2004). UCSF chimera—A visualization system for exploratory research and analysis. *Journal of Computational Chemistry*, 25, 1605–1612. <https://doi.org/10.1002/jccc.20084>
- Rimel, J. K., & Taatjes, D. J. (2018). The essential and multifunctional TFIIH complex. *Protein Science*, 27, 1018–1037. <https://doi.org/10.1002/pro.3424>
- Schneider, C. A., Rasband, W. S., & Eliceiri, K. W. (2012). NIH Image to ImageJ: 25 years of image analysis. *Nature Methods*, 9(7), 671–675. <https://doi.org/10.1038/nmeth.2089>
- Stefanini, M., Fawcett, H., Botta, E., Nardo, T., & Lehmann, A. R. (1996). Genetic analysis of twenty-two patients with Cockayne syndrome. *Human Genetics*, 97, 418–423. <https://doi.org/10.1007/BF02267059>
- Stefanini, M., Giliani, S., Nardo, T., Marinoni, S., Nazzaro, V., Rizzo, R., & Trevisan, G. (1992). DNA repair investigations in nine Italian patients affected by trichothiodystrophy. *Mutation Research/DNA Repair*, 273, 119–125. [https://doi.org/10.1016/0921-8777\(92\)90073-c](https://doi.org/10.1016/0921-8777(92)90073-c)
- Stefanini, M., Lagomarsini, P., Arlett, C. F., Marinoni, S., Borroni, C., Crovato, F., Trevisan, G., Cordone, G., & Nuzzo, F. (1986). Xeroderma-Pigmentosum (Complementation Group-D) mutation is present in patients affected by trichothiodystrophy with photosensitivity. *Human Genetics*, 74, 107–112. <https://doi.org/10.1007/BF00282072>. <https://107-112>
- Stefanini, M., Lagomarsini, P., Giliani, S., Nardo, T., Botta, E., Peserico, A., Kleijer, W. J., Lehmann, A. R., & Sarasin, A. (1993). Genetic heterogeneity of the excision repair defect associated with trichothiodystrophy. *Carcinogenesis*, 14, 1101–1105. <https://doi.org/10.1093/carcin/14.6.1101>
- Taylor, E. M., Broughton, B. C., Botta, E., Stefanini, M., Sarasin, A., Jaspers, N. G. J., Fawcett, H., Harcourt, S. A., Arlett, C. F., & Lehmann, A. R. (1997). Xeroderma pigmentosum and trichothiodystrophy are associated with different mutations in the XPD (ERCC2) repair/transcription gene. *Proceedings of the National Academy of Sciences*, 94, 8658–8663. <https://doi.org/10.1073/pnas.94.16.8658>
- Theil, A. F., Mandemaker, I. K., van den Akker, E., Swagemakers, S. M. A., Raams, A., Wüst, T., Martelijn, J. A., Giltay, J. C., Colombijn, R. M., Moog, U., Kotzaeridou, U., Ghazvini, M., von Lindern, M., Hoeijmakers, J. H. J., Jaspers, N. G. J., van der Spek, P. J., & Vermeulen, W. (2017). Trichothiodystrophy causative TFIIIE β mutation affects transcription in highly differentiated tissue. *Human Molecular Genetics*, 26, 4689–4698. <https://doi.org/10.1093/hmg/ddx351>
- Tsutakawa, S. E., Tsai, C. L., Yan, C., Bralić, A., Chazin, W. J., Hamdan, S. M., Schärer, O. D., Ivanov, I., & Tainer, J. A. (2020). Envisioning how the prototypic molecular machine TFIIH functions in transcription initiation and DNA repair. *DNA Repair*, 96, 102972. <https://doi.org/10.1016/j.dnarep.2020.102972>
- Ueda, T., Compe, E., Catez, P., Kraemer, K. H., & Egly, J. M. (2009). Both XPD alleles contribute to the phenotype of compound heterozygote xeroderma pigmentosum patients. *Journal of Experimental Medicine*, 206, 3031–3046. <https://doi.org/10.1084/jem.20091892>
- Ulloa-Aguirre, A., Janovick, J. A., Brothers, S. P., & Conn, P. M. (2004). Pharmacologic rescue of conformationally-defective proteins: Implications for the treatment of human disease. *Traffic*, 5, 821–837. <https://doi.org/10.1111/j.1600-0854.2004.00232.x>
- Vermeulen, W., Bergmann, E., Auriol, J., Rademakers, S., Frit, P., Appeldoorn, E., Hoeijmakers, J. H. J., & Egly, J. M. (2000). Sublimiting concentration of TFIIH transcription/DNA repair factor causes TTD—A trichothiodystrophy disorder. *Nature Genetics*, 26, 307–313. <https://doi.org/10.1038/81603>

- Vermeulen, W., Rademakers, S., Jaspers, N. G. J., Appeldoorn, E., Raams, A., Klein, B., Kleijer, W. J., Kjærsgård Hansen, L., & Hoeijmakers, J. H. J. (2001). A temperature-sensitive disorder in basal transcription and DNA repair in humans. *Nature Genetics*, 27, 299–303. <https://doi.org/10.1038/85864>
- Viprakasit, V., Gibbons, R. J., Broughton, B. C., Tolmie, J. L., Brown, D., Lunt, P., Winter, R. M., Marinoni, S., Stefanini, M., Brueton, L., Lehmann, A. R., & Higgs, D. R. (2001). Mutations in the general transcription factor TFIIF result in beta-thalassaemia in individuals with trichothiodystrophy. *Human Molecular Genetics*, 10, 2797–2802. <https://doi.org/10.1093/hmg/10.24.2797>
- Yan, C., Dodd, T., He, Y., Tainer, J. A., Tsutakawa, S. E., & Ivanov, I. (2019). Transcription preinitiation complex structure and dynamics provide insight into genetic diseases. *Nature Structural & Molecular Biology*, 26, 397–406. <https://doi.org/10.1038/s41594-019-0220-3>

SUPPORTING INFORMATION

Additional supporting information can be found online in the Supporting Information section at the end of this article.

How to cite this article: Lanzafame, M., Nardo, T., Ricotti, R., Pantaleoni, C., D'Arrigo, S., Stanzial, F., Benedicenti, F., Thomas, M. A., Stefanini, M., Orioli, D., & Botta, E. (2022). TFIIF stabilization recovers the DNA repair and transcription dysfunctions in thermo-sensitive trichothiodystrophy. *Human Mutation*, 1–12. <https://doi.org/10.1002/humu.24488>